*Proceedings of the Korean Nuclear Society Spring Meeting*

*Kwangju, Korea, May 1997*

# Experimental Study and Correlation Development of Critical Heat Flux under Low Pressure and Low Flow Condition

Hong-Chae Kim, Won-Pil Baek, Han-Kon Kim and Soon Heung Chang

Department of Nuclear Engineering

Korea Advanced Institute of Science and Technology

**ABSTRACT**

To investigate parametric effect on CHF and to get CHF data, experimental study has been performed with vertical round tubes under the condition of low pressure and low flow (LPLF). Test sections are made of Inconel-625 tube and have the geometry of 8 and 10 mm in diameter, and 0.5 and 1.0 m in heated length. All experiments have been conducted at the pressure of under 9 bar, the mass flux of under 250 kg/m$^2$s and the inlet subcooling of 350 and 450 kJ/kg, for stable upward flow with water as a coolant. Flow regime analysis has been performed for obtained CHF data with Mishima's flow regime map, which reveals that most of the CHF occur in the annular-mist flow regime. General parametric trends of the collected CHF data are consistent with those of previous studies. However, for the pressure effect on CHF, two different trends are observed; For relatively high mass flux, CHF increases with pressure and for lower mass flux, CHF decrease with pressure. Using modern data regression tool, ACE algorithm, two new CHF correlations for LPLF condition are developed based on local condition and inlet condition, respectively. The developed CHF correlations show better prediction accuracy compared with existing CHF prediction methods.

## 1. Introduction

Recently, interests on CHF for LPLF condition are increasing for the improved safety analysis of water-cooled reactor and for the development of the high heat flux removal system and advanced reactor using passive safety concept. In the case of loss of coolant accident (LOCA) in nuclear power plant, the mass flow rate may decrease considerably to values close to zero and even flow stagnation and flow inversion can take place in the circumstance of low pressure. In the advanced reactor, natural circulation that generally has low mass flow rate is very important mechanism for the passive safety component. Contrary to the high pressure and high flow (HPHF), there haven't been active experimental studies on CHF at LPLF condition, so available empirical data are too scarce to understand CHF characteristics and to make reliable CHF prediction methods at this condition.

Different from the HPHF condition, at LPLF condition, the effect of buoyancy force becomes remarkable because of the low flow rate and the flow becomes less stable because of large specific volume of steam at low pressure. This has been a main difficulty in understanding CHF at LPLF condition. There are many CHF prediction methods that cover the range of LPLF condition, but for the rack of the experimental data their reliability is not clear. In general, prediction errors of those methods become larger as mass flux and pressure getting lower. Especially the CHF behavior with pressure is very different for each prediction method. While more and more experimental studies dealing with LPLF CHF in vertical tube have been conducted, most of the experiments were performed at atmospheric pressure. Therefore more empirical LPLF CHF data are needed for the observation of the pressure effect on CHF, development of the more accurate CHF prediction methods and assessment of the existing correlations and look-up table. For the purpose of this, present experimental study has been carried out to improve understanding of the CHF behavior at LPLF condition with parameters affecting CHF, especially pressure, to get more CHF data for the extension of the experimental data bank, and to make more reliable CHF correlation. For the development of CHF correlation, alternating conditional expectation (ACE) algorithm has been used. ACE method is a generalized regression algorithm that yields an optimal relation between a dependent variable and multiple independent variables, and it is very useful for the sensitivity study of parameters because it doesn't need initial selection of the functional forms. In this study, two types of CHF correlation have been developed using ACE algorithm.

## 2. Background

Mishima et al. [1 ~ 4] performed a series of experiments for three different channel geometry with an internally heated annulus, two rectangular channels and a round tube. They analyze the effect of channel geometry, unheated wall and flow stability on CHF. One of the notable descriptions of their results is that the effect of inlet subcooling appears when mass flux exceeds about 200 $kg/m^2s$ for the vertical round tube. Chang et al. [5] performed CHF experiments with vertical round tubes for up and down flow at low mass flux ( $\leq$ 220 $kg/m^2s$ ) and developed LPLF CHF correlation based on flooding-limited CHF with their data and other's available data. They described that the local condition-type correlation using the thermodynamic equilibrium quality was not adequate for the LPLF CHF. Weber-Johanssen [6] accomplished temperature controlled CHF experiment with short vertical round tube ( L/D = 4.47 ) at low pressure ( $\leq$ 12 bar ) and low flow ( $\leq$ 300 $kg/m^2s$ ). With their data and others data, they developed LPLF CHF correlation based on Katto's CHF correlation. Besides these studies, many authors (Bowring [7], Katto [8], Shah [9], Groenoveld et al. [10]) developed CHF correlations and look-up table available at LPLF condition

For the understanding of the CHF characteristics, parametric trends of CHF are very important, however, pressure effect on CHF condition is not clear at LPLF condition. Moon et al. [11] investigated the CHF behavior by applying artificial neural networks (ANNs) to CHF data bank for upward flow of water in uniformly heated vertical round tubes. According to their study, the pressure effect seems to be complex. In overall, the CHF increase with pressure at low pressure, passes a maximum, then decrease at higher pressures. From their results, it can be easily noticed that system pressure effect for fixed inlet conditions is not clear especially under 10 bar which are the very conditions for investigation in this study. Collier et al. [12] illustrated the pressure effect at high mass flux (2720 $kg/m^2s$) with Bowring correlation. According to them, for the condition where the inlet subcooling is held constant, the CHF increase to a maximum at low pressure (below 30 bar) and then falls with pressure. Teyssedou et al. [13] performed CHF experiments for vertical up flow with round tube at low and medium pressures (5 ~ 30 bar) and high mass flux (1000 ~ 6000 $kg/m^2s$). They used tubes of 8 mm inner diameter and 0.75 ~ 1.8 m heated length and depicted the pressure effect: for longer tube ( $\geq$ 1 m ), CHF increases with pressure and for shorter tube ( = 0.75 m), CHF is observed to increase with pressure to 10 bar and then decrease.

## 3. Experiment

For the flow boiling CHF experiments under the condition of low pressure and low flow, test loop which can be pressurized up to 9 bar was constructed. Experimental loop consists of round tube type test section, once-through type condenser, pressurizer connected to the upstream of condenser, centrifugal pump, turbine flow meter, ball and needle valves and two series of preheaters. As a working fluid of the loop, water which was ion-exchanged by filter and distilled by preheater and test section before main experiment was used. Inlet temperature of test section was kept constant with two series of preheaters controlled automatically. To pressurize the loop, nitrogen gas was injected to the upper part of the pressurizer which provided compressible volume to the loop for maintaining desired pressure value.

Test section was made of Inconel-625 round tube whose electrical and mechanical characteristics were well approved. Four types of tubes with inner diameter of 8 and 10 mm and length of 0.5 and 1.0 m were used as a heated section. Three Type-K thermocouples were attached on the test section outer surface by thermocouple clamp to check sudden temperature increase that is an indication of the CHF occurrence. A pair of clamp type copper electrodes grabbed both ends of the test tube to provide electrical power and the test section was heated by Joule heating.

Flow rate was measured by turbine flow meter (0.1 ~ 1.0 l/min) and mass flux was calculated in real time using flow meter inlet temperature and pressure. Voltage signals from flow meter, thermocouples, pressure tap were obtained by HP 3852A Data Acquisition/Control units, and were recorded and processed by IBM PC/586.

Experiments have been performed for upward flow of water with different pressure and mass flux. Inlet subcooling was fixed nearly same condition with two preheater. One of them has a cooler for the condition of excess temperature increase in inlet of test section. Flow rate was controlled by two needle valves located at the upstream of flow meter and test section inlet. After setting inlet subcooling, mass flux, and test section outlet pressure at desired value, heat flux was increased with enough duration time for stabilization of other experiment parameters. CHF point was defined as the condition where the maximum wall temperature of the test section increase suddenly with the increase rate over 50°C.

The experimental errors involved in the measurements are estimated at ± 1.6 °C for the Type-K thermocouples, ± 1.5 °C for the Type-T thermocouples, ± 1 kPa for the pressure tab, ± 3 % for the mass flux, and ± 5 % for the heat flux.

## 4. Experimental Results and Discussion

*4.1 Flow regime analysis*

174 CHF data were obtained from this experimental study at the various pressure conditions under 9 bar. Because flow pattern of the two-phase flow in the test section is a very important factor for the CHF phenomena, CHF data obtained from this study were classified and analyzed with the Mishima [14]'s flow regime map. In Fig. 1 ~ 2, the CHF data were plotted on flow regime map at the pressure of 2 bar and 7 bar for the diameter of 8 mm. Line (1) shows the entrainment induced flow transition suggested by Mishima and line (2) and (3) are entrainment initiation boundaries developed by Govan et al.[15] and Steen[16], respecively. An investigation of these figures reveals that the most of the CHF data are included in annular-mist flow regime where liquid flows on the wall in the form of film with a liquid droplet in the steam core. As mass flux decreases, the CHF data move to annular flow regime.

So, it can be thought that CHF at LPLF is mainly governed by entrainment which is a function of surface tension and density of steam. However, as mass flux decreases to very low value, flow pattern at CHF condition moves to annular region, which means that little or no entrainment will take place at low mass flux.

*4.2 Parametric Trend of CHF*

As a complex phenomenon affected by many parameters, CHF behaves differently with each parameter. Trends of the obtained CHF data are analyzed with mass flux, inlet subcooling, heated length and tube inner diameter in the view of fixed inlet condition.

*Mass flux effect* : As generally known CHF increases with mass flux, however, the increase rate decreases with increasing mass flux. As heated length getting shorter, mass flux effect becomes larger. Mass flux effect becomes larger with the increase of diameter.

*Inlet subcooling effect* : In Fig. 3 ~ 4, inlet subcooling effect is shown with pressure. CHF increases with increasing inlet subcooling and increase rate of it becomes larger as mass flux increases. This increasing trend is different from other studies. Mishima et al. and Chang et al. described that the effect of inlet subcooling disappears when mass flux is under 200 and 190kg/m$^2$s respectively. However, in this study, inlet subcooling effect appears even at 60 kg/m$^2$s.

*Heated length and diameter effect* : As generally known CHF decrease with increase of heated length and increase with increase of diameter.

*Pressure effect* : As referred previously, pressure effect on CHF at LPLF is somewhat complex. CHF data are plotted in Fig. 3 ~ 4 with pressure. From these figures, the following observations can be made for the range of parameters investigated.

1. For a relatively large mass flux ($\geq$150 kg/m$^2$s), the CHF increases with increasing pressure.
2. For a relatively small mass flux ($\leq$100 kg/m$^2$s), the CHF decreases or is nearly same with increasing pressure, except the case of the short tube (0.5 m).

For the explanation of those opposite CHF trends with pressure, water and steam properties are investigated. As pressure increases, surface tension, latent heat of vaporization and steam-to-water specific volume ratio decrease. Especially, the specific volume ratio sharply decreases (up to about 30 bar), and then it is nearly constant with increasing pressure. This can explain the general CHF trend with pressure: CHF increases to a maximum and then decreases.

In low pressure (under 30 bar) condition the increase of CHF with pressure can be explained with very high specific volume ratio. In this condition, flow instability due to high specific volume ratio is dominant CHF occurrence mechanism. As pressure increases from atmospheric to 30 bar, flow instability becomes less resulting decrease in mechanical entrainment and premature liquid film break. This leads higher CHF as pressure becomes higher.

In high pressure (over 30 bar) condition where the specific volume ratio is nearly constant, the decrease of CHF with pressure can be explained with the domination of the surface tension and latent heat of vaporization effects on CHF. As pressure increases, the liquid film becomes thin because of the lower latent heat of vaporization and lower surface tension which results unstable liquid film surface. This phenomena decrease CHF as pressure increases.

But, general CHF trend with pressure becomes different when mass flux is very low. This behavior can be explained using the flow regime map. As shown in Fig. 3 ~ 4, most of the CHF at very low flow ($\leq$ 60 kg/m$^2$s) is in or near annular regime, where little or no entrainment occurs because of the low flow rate of liquid film. Therefore, at very low flow condition, latent heat is the dominant factor and CHF just decreases (not increase to some peak value) with increase of pressure for all range because of lower latent heat of vaporization, lower surface tension and weak entrainment effect.

### 5. Advanced LPLF CHF Correlation Development

The ACE algorithm [17] is a modern data regression tool using various statistical estimators such as mean, standard deviation, covariance, and so on. Thus, it is desirable for input data set to have statistically meaningful distribution such as normal or uniform distributions for the governing parameters. In this study, CHF data are gained under the condition of only two inlet subcooling (350 and 450 kJ/kg), two tube diameter (8 and 10 mm) and two heated length (0.5 and 1.0 m). Therefore CHF data show undesirable distribution. To solve this problem, CHF data under the condition of low pressure ($\leq$ 11 bar) and low mass flux ($\leq$ 500 kg/m$^2$s) are selected from the KAIST CHF data bank. However, most of the LPLF CHF experiments were conducted near the atmospheric pressure which making bad parametric distribution for pressure. Thus, the CHF data obtained at atmospheric pressure were discarded resulting 442 CHF data including this study's data for better data distribution. In the case of exit condition correlation development, 127 data having the heated length to diameter ratio less than 80 are deleted to exclude the heated length effect.

Based on Ahmad [18]'s dimensionless parameters, 6 and 7 dimensionless parameters for exit and inlet conditions are selected through sensitivity study with ACE algorithm and modification. From the sensitivity study, Froud-Reynolds number, Prandtl number and thermal conductivity ratio are dropped because of the weak effect on CHF, which mean that gravity effect, heat convection and heat conduction is not important at LPLF CHF condition. With the selected dimensionless parameters, following two LPLF CHF correlations were developed.

For the exit condition, following correlation was obtained based on the 315 CHF data with parametric ranges: $0.00776 \leq D$ (m) $\leq 0.01310$, $0.960 \leq L$ (m) $\leq 3.120$, $110 \leq P$ (kPa) $\leq 1089$, $49.2 \leq G$ (kg/m$^2$s) $\leq 499.0$, $0.462 \leq X \leq 0.990$.

$$q_c = \left[\frac{\sigma\rho_f}{G^2 L}\right]^{2.1961} \left[\frac{\mu_f}{GD}\right]^{0.8967} \left[\frac{GD}{\mu_g}\right]^{4.7112} \exp\left[-52.8501 + 26.4633\left(\frac{\rho_g}{\rho_f}\right)^{0.3}\right](1-X)^{0.5282} G h_{fg} \qquad \text{(Eq. 1)}$$

For the inlet condition, following correlation was suggested based on the 442 CHF data with parametric ranges: $0.00457 \leq D$ (m) $\leq 0.01310$, $0.043 \leq L$ (m) $\leq 3.120$, $110 \leq P$ (kPa) $\leq 1098$, $13.0 \leq G$ (kg/m$^2$s) $\leq 499.0$, $13.0 \leq \Delta h_i \leq 684.0$.

$$q_c = 0.00226\left[\frac{\sigma\rho_f}{G^2 L}\right]^{0.3629} \left[\frac{GD}{\mu_f}\right]^{0.6293} \left[\frac{\mu_g}{GD}\right]^{0.1021} \left[0.0273 + \frac{\Delta h_i}{h_{fg}}\right]^{0.1911} \left[\frac{\rho_g}{\rho_f}\right]^{0.0279} \left[\frac{D}{L}\right]^{0.3857} G h_{fg} \qquad \text{(Eq. 2)}$$

Developed LPLF CHF correlations (Eq. 1 & 2) are assessed with the 315 data used in exit type correlation development and the results are shown in Table 1. Because Eq. 1 is a local condition type correlation, two kinds of assessment method, direct substitution method (DSM) and heat balance method (HBM) are applied to know prediction accuracy. For the DSM, it doesn't show good prediction accuracy giving average error of 1.2 % and RMS error of 38.1 %. However this result is fairly good compared to existing local condition type CHF prediction method, AECL 1995 look-up table, which shows average error of 29.2 % and RMS error of 76.8 %. For the HBM, Eq. 1 shows quite good prediction accuracy with average error of –0.5 % and RMS error of 10.2 %. For inlet type correlations, Eq. 2 shows the best prediction accuracy with average error of –0.3 % and RMS error of 8.3 % among other CHF prediction methods. Assessment result of other CHF prediction methods are also shown in Table 1.

For the 442 CHF data, Eg. 2 shows average error of 0.3 % and RMS error of 15.0 %. These errors are nearly two times greater than that for 315 data. This can be explained with flow regime; most of the data which have L/D ( $\leq$ 80 ) in 442 data were Weber's data obtained with very short tube ( L = 43 mm ). In this condition flow regime is not annular or annular-mist flow while in other conditions, flow regime is annular or annular-mist flow. Therefore it can be concluded that Eq. 2 should be used for only annular or annular-mist flow for better accuracy.

Notable point from the assessment results is that the application of local type CHF prediction with DSM is not appropriate for LPLF CHF.

## 6. Conclusion

The experimental study of CHF was carried out under the condition of low pressure (≤ 9 bar) and low mass flux (≤ 250 kg/m$^2$s). The experiments were conducted for two heated lengths (0.5, 1.0 m) with Inconel-625 tubes having two inner diameter of 8 and 10 mm. 174 CHF data are obtained for vertical round tube at stable upward flow condition and more accurate CHF correlations were proposed.

Important results are as follows:

1. The flow regime analysis was conducted for experimental CHF data using Mishima's flow regime map. It shows that CHF at LPLF are taken place in annular-mist flow regime except very low flow condition.
2. The observed parametric trends of CHF data based on fixed inlet conditions generally agree with those of previous studies except pressure effect. CHF increases with increasing mass flux, diameter and inlet subcooling, but CHF decrease with increasing heated length.
3. The effect of pressure on CHF was investigated and shows following two opposite results;
   - For a relatively large mass flux (≥ 150 kg/m$^2$s), the CHF increases with pressure.
   - For a relatively small mass flux (≤ 100 kg/m$^2$s), the CHF decreases or is nearly same with pressure, except the case of the short heated length (0.5m).
4. Using ACE algorithm, two CHF correlations based on exit and inlet condition were developed with obtained CHF data and other available CHF data from KAIST CHF data bank. Developed CHF correlations give reasonable prediction accuracy. Especially, inlet condition type correlation shows best prediction ability among other CHF prediction method in annular and annular-mist flow regime and it can be very useful for LPLF CHF condition.

## References


1. K. Mishima and H. Nishihara, The effect of flow direction and magnitude on CHF for low pressure water in thin rectangular channels, *Nucl. Eng. Des.* **86**, 165-181 (1985).
2. K. Mishima, H. Nishihara and I. Michiyoshi, Boiling burnout and flow instabilities for water flowing in a round tube under atmospheric pressure, *Int. J. Heat Mass Transfer* **28**[6], 1115-1129 (1985).
3. K. Mishima and H. Nishihara, Effect of channel geometry on critical heat flux for low pressure water, *Int. J. Heat Mass Transfer* **30**[6], 1169-1182 (1987).
4. K. Mishma, H. Nishihara, M. Kureta and K. Tasaka, Critical heat flux for low pressure water in small diameter tubes, *Proc. 6$^{th}$ Int. Top. Meet. Nucl. Reactor T/H*, pp. 435-443, Grenoble (1993).
5. S. H. Chang, W. P. Baek and T. M. Bae, A study of critical heat flux for low flow of water in vertical round tubes under low pressure, *Nucl. Eng. Des.* **132**, 225-237 (1991).
6. P. Weber and K. Johannsen, Study of critical heat flux condition at convective boiling of water: temperature and power controlled experiments, *Proc. 9$^{th}$ Int. Heat Transfer Conf.*, Jerusalem, **2**, 63-68 Paper No. 1-BO-11 (1990).
7. R. W. Bowring, A Simple But Accurate Round Tube Uniform Heat Flux, Dryout Correlation Over the Pressure Range 0.7-1.7 MN/m$^2$ (100-2500 psia), AEEW-R 789 (1972).
8. Y. Katto and H. Ohno, An improved version of the generalized correlation of critical heat flux for the forced convective boiling in uniformly heated vertical tubes, *Int. J. Heat Mass Transfer* **27**[9], 1641-1648 (1984).
9. M. M. Shah, Improved general correlation for critical heat flux during upflow in uniformly heated vertical tubes, *Heat and Fluid Flow* **8**[4], 326-335 (1987).
10. D. C. Groenoveld, L. K. H. Leung, P. L. Kirillov, V. P. Bobkov, I. P. Smogalev, V. N. Vinogradov, X. C. Huang and E. Royer, The 1995 look-up table for critical heat flux in tubes, *Nucl. Eng. Des.* **163**, 1-23 (1996).
11. S. K. Moon, W. P. Baek, S. H. Chang, Parametric trends analysis of the critical heat flux based on artificial neural networks, *Nucl. Eng. Des.* **163**, 29-49 (1996).
12. J. G. Collier and J. R. Thome. Convective Boiling and Condensation (3rd Ed.), pp. 329-367, Oxford University Press (1994).
13. A. Teyssedou, A. Olekhnowitch, A. Tapucu. Champagne and D. Groenoveld, Critical heat flux data in a vertical tube at low and medium pressures, *Nucl. Eng. Des.* **149**, 185-194 (1994).
14. K Mishima, Flow regime transition criteria for upward two-phase flow in vertical tubes, *Int. J. Heat Mass Transfer* **27**[5], 723-737 (1984).
15. A. H. Govan, G. F. Hewitt, D. G. Owen and T. R. Bott, An improved CHF modeling code, *2$^{nd}$ UK National Conference on Heat Transfer*, London, **1**, 33-48 (1988).
16. G. B. Wallis, One dimensional two-phase flow, McGraw-Hill (1969).
17. L. Breiman and J. H. Friedman, Estimating optimal transformations for multiple regression and correlation, *Journal of the American Statistical Association, Thoery and Method* **80**[391], 580-601 (1985).
18. S. Y. Ahmad, Fluid to fluid modeling of critical heat flux: A compensated distortion model, *Int. J. Heat Mass Transfer* **16**, 641-662 (1973).

Table 1. Assessment results of CHF correlations and look-up table

| Correlation type | Table/Correlation | Assessment method | No. Data | Avg. error (%) | RMS error (%) |
|---|---|---|---|---|---|
| Local type | AECL 1995 | DSM | 315 | 29.1 | 76.8 |
| | | HBM | 315 | 3.6 | 12.0 |
| | Eq. 1 | DSM | 315 | 1.2 | 38.1 |
| | | HBM | 315 | -0.5 | 10.2 |
| Inlet type | Eq. 2 | Fixed inlet | 315 | -0.3 | 8.3 |
| | Bowring | Fixed inlet | 286 | 6.3 | 11.1 |
| | KAIST 95 | Fixed inlet | 283 | -0.7 | 17.5 |
| | Katto | Fixed inlet | 315 | 20.5 | 25.3 |
| | Weber-Johannsen | Fixed inlet | 155 | 11.8 | 21.8 |
| Mixed type | Shah | Fixed inlet | 315 | -2.0 | 10.3 |

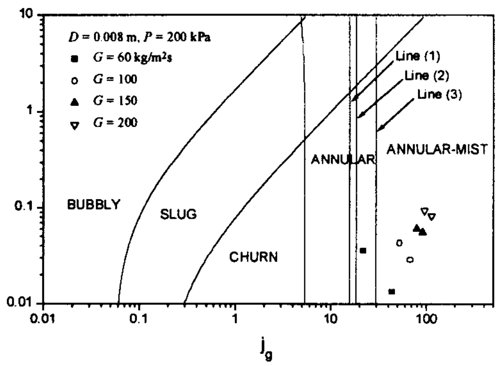

Fig. 1. Flow regime of the data for D=0.008 m and P = 200 kPa

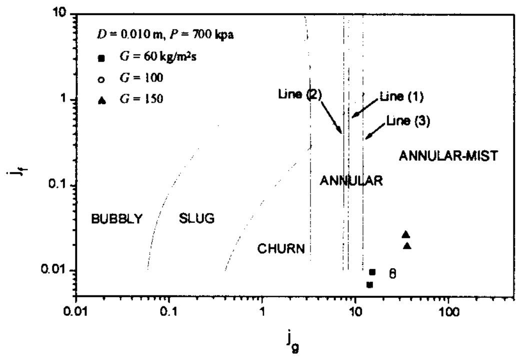

Fig. 2. Flow regime of the data for D=0.008 m and P = 700 kpa.

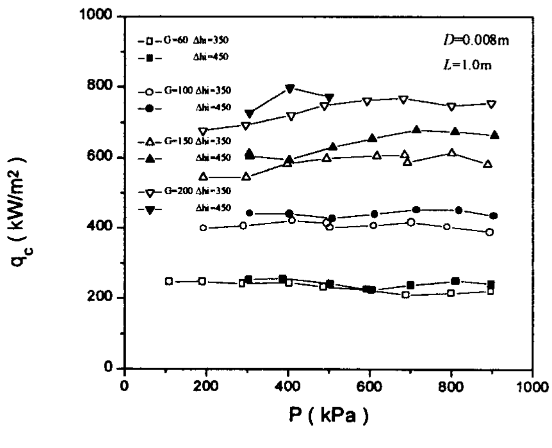

Fig. 3. Pressure effect on CHF for D=0.008 m and L=1.0 m

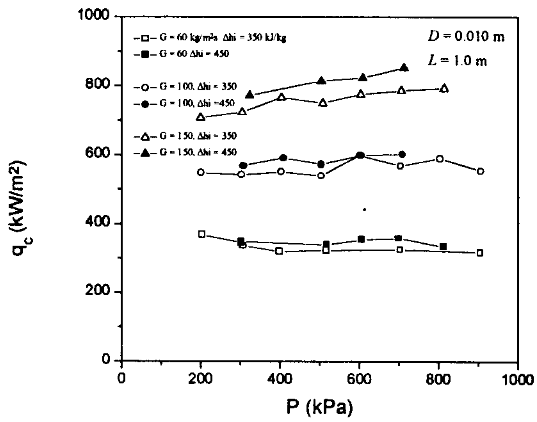

Fig. 4. Pressure effect on CHF for D=0.010 m and L=1.0 m